UNIVERSITY OF CALIFORNIA SAN DIEGO

Reverse Localization of Wi-Fi Access Points

A Thesis submitted in partial satisfaction of the
requirements for the degree
Master of Science

in

Electrical and Computer Engineering (with a specialization in Communication Theory and Systems)

by

Aravind Seetharaman

Committee in charge:

Professor Dinesh Bharadia, Chair
Professor Nikolay Atanasov
Professor Xinyu Zhang

2019

The thesis of Aravind Seetharaman is approved, and it is acceptable in quality and form for publication on microfilm and electronically:

_____

_____

_____

Chair

University of California San Diego

2019

DEDICATION

To my mother, who has always put me before everything else. To my father, watching from the stars.

TABLE OF CONTENTS

Signature Page . . . iii

Dedication . . . iv

Table of Contents . . . v

List of Figures . . . vii

Acknowledgements . . . viii

Abstract of the Thesis . . . ix

Chapter 1 Introduction . . . 1
1.1 Need for Reverse Localization . . . 1
1.2 Related Work on Wi-Fi Localization . . . 3

Chapter 2 Primer on CSI and Wi-Fi based Localization . . . 6
2.1 Channel State Information (CSI) . . . 6
2.2 Wi-Fi Localization Primer . . . 7

Chapter 3 Reverse Localization of an Access Point . . . 10
3.1 Contributions . . . 10
3.2 Assumptions . . . 11
3.3 Reverse Localization Algorithm . . . 11

Chapter 4 Determination of AP Orientation and Antenna Separation . . . 17

Chapter 5 Experimental Setup and Evaluation . . . 23
5.1 Requirements . . . 23
5.1.1 SLAM Algorithm . . . 24
5.1.2 Turtlebot 3 . . . 24
5.2 Reverse Localization Procedure and Evaluation . . . 27
5.2.1 Data Collection and Reverse Localization . . . 27
5.2.2 Results . . . 28
5.3 AP Geometry Prediction Results . . . 30
5.4 Error in Reported Ground Truth . . . 31

Chapter 6 Conclusion and Future Work . . . 33
6.1 Summary . . . 33
6.2 Future Work . . . 33
6.3 Applications . . . 34

Bibliography 35

LIST OF FIGURES

Figure 1.1: Conventional Wi-Fi Localization using Triangulation 4

Figure 2.1: Presence and Absence of Direct Path 9

Figure 3.1: Robot traversing an unknown environment 11
Figure 3.2: Robot Mapping Process Flow 12
Figure 3.3: Variation in localization error with respect to AP Location error 13
Figure 3.4: Variation in median localization error, with number of APs 13
Figure 3.5: Simulating multiple Access Points 14
Figure 3.6: Variation in localization error with respect to Antenna Separation error . . 16

Figure 4.1: Closed form solution 18
Figure 4.2: Estimating AoD from phase difference 19
Figure 4.3: Estimating AoD from rate of change of phase difference 20

Figure 5.1: Turtlebot with Quantenna 25
Figure 5.2: Reverse Localization Accuracy Results 28
Figure 5.3: Reverse Localization Accuracy for different number of antennas 29
Figure 5.4: Reverse Localization Accuracy for different bandwidths 30
Figure 5.5: CDF Plot of error in predicted d 31
Figure 5.6: Ground Truth Error CDF plot 31

ACKNOWLEDGEMENTS

God, for all the opportunities that he has given me, to the point where I sometimes find myself wondering if I deserve so much.

My parents, grandparents, relatives and friends who have always believed in me and stood by me, through the good times and bad.

My advisor Dr. Dinesh Bharadia, for taking me under his wing. I had always had doubts about my aptitude for research, and he showed me that all it takes are deep interest and a lot of hard work. His help and feedback have been immensely valuable.

My project mates Shreya Ganesaraman and Shrivatsan Rajagopalan. I am not sure how I would have survived graduate school without them. The sleepless nights and hours of hard work were in a way, very good times.

My fellow WCSN members, especially Sai Roshan and Ish Jain, for their help, ideas and support. Some of the work that you are doing is definitely going to have a big impact in future.

My thesis committee members, Dr Xinyu Zhang and Dr Nikolay Atanasov for their insightful comments and feedback.

Chapters 1-6 are adapted from material currently being prepared for submission for publication with Ganesaraman, Shreya; Rajagopalan, Shrivatsan; Ayyalasomayajula, Sai Roshan; Jain, Ish Kumar; Bharadia, Dinesh.

ABSTRACT OF THE THESIS

Reverse Localization of Wi-Fi Access Points

by

Aravind Seetharaman

Master of Science in Electrical and Computer Engineering (with a specialization in Communication Theory and Systems)

University of California San Diego, 2019

Professor Dinesh Bharadia, Chair

This thesis presents the design of a reverse localization system that works to accurately localize the individual antennas of all WiFi access points deployed in a target region. This would enable the localized access points to localize themselves and in turn localize and provide navigation for any new mobile devices entering that network. In order to achieve this, a location aware mobile robot carrying an antenna array is moved to a number of known locations in the map to collect Channel State Information (CSI) from multiple randomly deployed access points present in the region. The information about the location of the robot and the CSI collected by the robot which by itself acts as a mobile access point, is used localize one antenna on the access point.

This reverse localization system's tracking algorithm uses phase differences between the localized antenna and the other antennas to identify the distance of separation between the antennas and the orientation of the antenna array present on the access point. Initial results provide centimeter accuracy for the location of the access point and millimeter level accuracy for the positions of the other antennas on the AP. This enables us to extend Wi-Fi based localization to various indoor environments.

Chapter 1

Introduction

1.1 Need for Reverse Localization

Outdoor localization accuracy has been constantly improving due to the advancements in Global Positioning System (GPS) technology [1]. They have improved to the extent where entire applications have been built based on GPS such as navigation apps [2], cab services [5], food delivery services etc. However, an ubiquitous indoor localization system is yet to be widely utilized like outdoor navigation systems and mobile apps. Indoor localization is projected to become a multi-billion dollar industry in the next few years. Due to the advent of various applications such as augmented and virtual reality, dynamic sensor networks, mobile e-commerce etc., a highly accurate indoor localization system is a necessity in order to bring about further advancements [36] in mobile computing and Internet of Things (IoT) applications. Also, indoor localization can be a useful tool in the case of indoor navigation as well, in large public buildings such as shopping malls, airports, and even in industrial applications such as warehouses etc.

GPS location estimates can become very inaccurate in indoor environments [28, 37] due to a plethora of reasons. GPS signals are at their most accurate when it comes to Line of Sight (LoS) scenarios, which can be obtained between the user and the GPS satellite outdoors. However,

when the user is present in an indoor location, the frequency at which GPS signals are transmitted are not able to penetrate thick objects such as walls. Due to this, GPS based indoor localization is not an option. Wi-Fi based localization has been in development as a possible solution for this problem for the past few years. However, it does not entirely solve the problem of indoor localization due to a number of factors. Most importantly, Wi-Fi based localization systems make these two key assumptions:

- The floor map and features of the indoor environment are known previously.
- The exact locations of the Wi-Fi Access Points are known and marked on the floor map of the said environment.

Usually all of these measurements are made by specialized equipment such as VICON [6] etc. This is a manual, labor-intensive and time-consuming process, especially in large environments. The key question that arises here is that, what if the environment was unknown? What if we had no knowledge about the map of the region, or the locations of the Access Points. This is where Wi-Fi based localization as such fails. More than just the locations of the APs, Wi-Fi based localization algorithms require even more information which are:

- How the Access Point is oriented in space?
- Where are the antennas present on the AP?
- What is the distance of separation between the antennas?

Thus, a system is required to ”Reverse Localize” all the Access Points present in a given region, determine their orientation in space and their antenna geometry. The ideal requirements for such a reverse localization system, after obtaining a map of the unknown region would be:

- Should be able to localize APs in the map of the region.

- Should have high level of localization accuracy, to the order of cm.
- Should be able to obtain the geometry of AP, to the order of mm.

1.2 Related Work on Wi-Fi Localization

There have been numerous Wi-Fi localization systems that have been developed. Early systems relied mainly on Received Signal Strength Indicator (RSSI) [11, 12, 27] , which mobile devices are able to measure. Using RSSI information from multiple APs, these systems are able to localize the user device. However, a major drawback is that these systems only provide an accuracy of a few meters, which can become even higher due to the fact that RSSI can vary greatly with changing environments, especially with multipath.

This less than desirable localization accuracy can be improved by using RSSI fingerprinting techniques [10, 32, 44, 35] . However, they are also at the mercy of the changing environmental conditions, which can still affect their localization efficiency. Therefore, a safe assumption to make is that RSSI systems are nearly not accurate enough for present-day systems and work effectively only under certain conditions as well. Many recent works also utilize RF back-scatter based indoor localization [8, 7, 18, 20, 21, 30, 29, 31, 41, 43, 45, 24], but this is also not possible to leverage in an unfamiliar environment.

With the advent of MIMO, another technique of Wi-Fi Localization was developed based on Angle of Arrival (AoA) estimates [19, 42, 25, 22, 11, 39, 40, 15, 26, 33, 38]. The main idea behind such techniques was to calculate the angles of arrival of all the multipath signals received at the multiple antennas present in the AP, and isolate the signal corresponding to the direct path between the target device and the AP. When this process is repeated at multiple APs, again triangulation can be done to localize the target. They provide sub-meter accuracy which is much more suited for modern applications, such as ArrayTrack[42] and Ubicarse[25]. However, a major drawback of many of these techniques is that they require hardware modifications[26, 42] in the

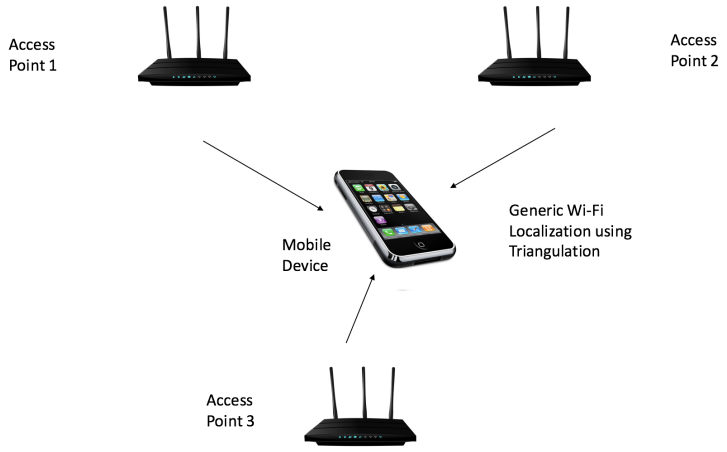

Figure 1.1: Conventional process of Wi-Fi localization using Triangulation

commodity APs, which may not always be possible. Also, these systems provide such levels of accuracy only if a large number of antennas are present (to the order of 8-16 antennas)[42]. This may not be suitable for commodity APs, and can cause deployment to be a significant issue. Position Tracking for VR has been achieved to the order of centimeter-level accuracy [23], but these systems assume significant multipath to be present in the environment for leverage, and achieve such levels of accuracy subsequently. These systems also assume that the antenna separation is lesser than $\lambda/2$, which is not always the case in commodity APs. Reverse Localization as a problem as such has been solved only by using Ultra Wide Band frequencies[13], which are not deployable in commodity hardware and requires specialized infrastructure.

More the number of APs present in the environment, the higher is the localization accuracy. However, if we require centimeter level precision, which is a major goal of the proposed system, we require a significant amount of Access Points to be present in the region, which is practically not possible. There are also time-based approaches, which make use of timestamps which are obtained from the Wi-Fi cards. The accuracy of these systems are also in the range of a few meters which is not exactly a marked improvement compared to previous systems. However, joint estimation of AoA and Time of Flight (ToF) can be extremely effective and improve the accuracy

of localization in scenarios where all the clocks of the Wi-Fi APs and devices connected to them are synchronized. But in practical cases, this is rarely the case. Thus, this is not a feasible option.

From all of these algorithms, some things which can be clearly observed are that a robust system with a high level of accuracy is required, and this system must be ideally implemented directly on commodity hardware without making any modifications because that may not be possible in many cases. Thus, Wi-Fi localization techniques, which leverage both AoA and ToF estimates are utilized, that can also be deployed directly on commodity APs. These techniques are used to reverse localize, and locate the position of the first antenna of the AP in question. After obtaining this location estimate, we need to solve for the antenna separation and geometry of the AP.

The system proposed in this thesis satisfies all of these aforementioned requirements, and is able to provide a solution built on a Robot Operating System (ROS) [3] based platform, and locate the Access Points present there.

Chapter 1 is adapted from material currently being prepared for submission for publication with Ganesaraman, Shreya; Rajagopalan, Shrivatsan; Ayyalasomayajula, Sai Roshan; Jain, Ish Kumar; Bharadia, Dinesh.

Chapter 2

Primer on CSI and Wi-Fi based Localization

2.1 Channel State Information (CSI)

When we consider the term Channel State Information (CSI), it can be defined as a coefficient of a wireless channel. Wi-Fi systems using OFDM report the CSI values as complex numbers. These complex numbers together constitute a CSI matrix, whose dimensions depend on the number of transmitting antennas, number of receiving antennas and the number of subcarriers. This means that there is a complex CSI value corresponding to every subcarrier, for every antenna in the system.

At a high level, CSI, as its name suggests gives us information about the transmission channel. Usually, CSI is computed at the receiver and then provided to the transmitter, though the inverse is also possible. The main information which we can obtain from the CSI, and also the information most relevant to localization is the attenuation and phase shift caused due to the environment in the channel. These parameters can be measured at each subcarrier of each antenna, and this is pretty much what the complex numbered CSI matrix represents.

This means that we can consider the CSI value at each subcarrier to be the sum of all the received multipath signals at each antenna in the receiver. The higher the number of antennas, the finer the CSI estimate is. However, as mentioned previously, this may not be possible with commodity hardware and hence we must make best use of the available CSI obtained from these. These CSI values and the corresponding CSI matrix can be obtained directly from commercial Wi-Fi cards and access points. Using this CSI information, we can estimate the Angle of Arrival (AoA) and Time of Flight (ToF) parameters which are required for Wi-Fi localization.

2.2 Wi-Fi Localization Primer

State-of-the-art Wi-Fi localization algorithms currently use key wireless channel properties like phase, amplitude, frequency, etc. by estimating the CSI of a user device at the access points present in the environment. Consider a scenario shown where we have one user transmitting at a specific wavelength, λ to an access point located L distance away. Then, the wireless channel measured at AP, h is given as follows:

$$h = \sum_{k=1}^{N} a_k e^{-\iota \frac{2\pi}{\lambda} L_k + \phi_e}, \tag{2.1}$$

where a_k is the attenuation constant for the k^{th} path when the signal is travelling across N different paths to reach the access point, c is the speed of light, ϕ_e is the error in phase added to the signal due to the channel, L_k is the distance travelled by the signal in k^{th} path and for one path (say 0), $L_0 = L$ corresponding to the direct path from the user to the access point. We can see that the signal travels an extra distance of $d \sin\theta$ to the second antenna with respect to the first antenna. Where d is the antenna separation and θ is the incident angle measured at the AP of the received signal with respect to the normal. Thus for multiple paths received at the access point

we have the measured channel at any i^{th} antenna, h_i as:

$$h_i = \sum_{k=1}^{N} a_k e^{-\iota \frac{2\pi}{\lambda}(L_k + (i-1)d\sin\theta_k + \phi_e)} \tag{2.2}$$

Where θ_k is the incident angle measured at the AP with respect to the normal for the k^{th} path among the N paths travelled by the signal. The equation (2.2) is for the channel measured for one wavelength or for one frequency carrier, while WiFi employs an OFDM modulation, where we have N_c frequency sub-carriers, thus extending our channel measured to $h_{i,j}$ as

$$h_{i,j} = \sum_{k=1}^{N} a_k e^{-\iota \frac{2\pi}{\lambda_j}(L_k + (i-1)d\sin\theta_k + \phi_e)} \tag{2.3}$$

Where λ_j is the wavelength of the j^{th} sub-carrier. We can observe that there are N distinct paths with N distinct solutions for θ and L in the given channel estimate $h_{i,j}$. We can isolate these paths by a simple 2D transform to obtain a likelihood profile, $\Lambda(\alpha_m, D_k)$ for a given θ and L, as described by the authors in [9] is as follows:

$$\Lambda(\alpha_m, l_k) = |\sum_{i=1}^{N_{ant}} \sum_{j=1}^{N_{sc}} h_{i,j} e^{\iota \frac{2\pi}{\lambda_j}(l_k + (i-1)d\sin\alpha_m)}| \tag{2.4}$$

Where N_{sc} is the number of sub-carrier frequencies and N_{ant} are the number of antennas on the access point. To identify the required angle of the direct path, we note that in [22], the authors make a distinct observation that the direct path travels the least distance from the user to the receiver. Based on this observation that the direct path has the least time-of-flight (ToF) we can measure the angle-of-arrival (AoA or θ_k) corresponding to the direct path.

One can observe that at this point we still do not consider the corresponding L_k as the direct path distance of the user measured from the access point, as the phase information is corrupted with initial phase offset, thus giving us a relative time-of-flight information instead of true time-of-flight information. So, many of the existing algorithms [22, 42] use this AoA

corresponding to direct path from multiple access points and triangulate the location of the user. Also, aggregating and utilizing AoA information obtained from multiple Access Points can be especially useful if the direct path between the Access Point and the user device is obscured by some obstacle such as walls etc. In that case, accuracy is compromised, and considering multiple APs will be the way to resolve this. Thus, we are ultimately able to locate the mobile device.

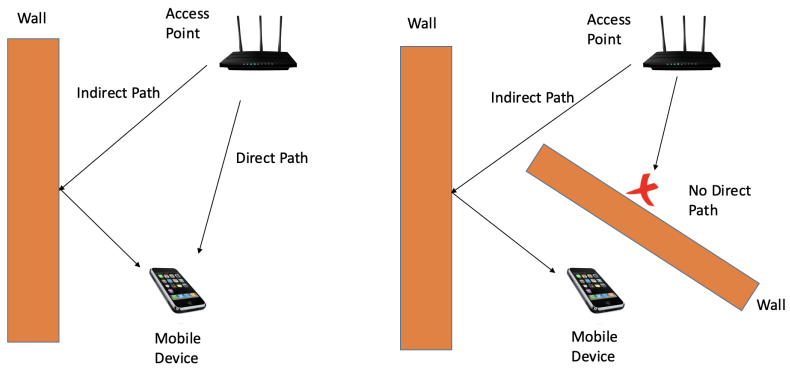

Figure 2.1: Left figure shows a scenario where a Direct Path is present in addition to the indirect path. The figure on the right shows a scenario where there is no direct path between the AP and the device.

Chapter 2 is adapted from material currently being prepared for submission for publication with Ganesaraman, Shreya; Rajagopalan, Shrivatsan; Ayyalasomayajula, Sai Roshan; Jain, Ish Kumar; Bharadia, Dinesh.

Chapter 3

Reverse Localization of an Access Point

By utilizing AoA and ToF information obtained from the CSI data, we can implement a Wi-Fi based localization system, which is able to reverse localize Wi-Fi Access Points as well. This chapter deals with the reverse localization algorithm.

3.1 Contributions

In order to solve the problem of reverse localization in an unknown environment, and provide the required levels of accuracy in localizing the AP and its geometry, we have designed a reverse localization system. The main contributions of the system are as follows:

- The system is able to reverse localize the Access Points present in the unknown environment, to the order of centimeter-level accuracy.
- The system is able to determine the antenna separation and thereby the locations of the antennas present on the AP, to the order of millimeter-level accuracy.
- The system is able to identify the geometry and orientation of the AP in the region, to the order of sub-10 degree accuracy.

3.2 Assumptions

For our implementation of the reverse localization system to localize the AP and determine its geometry, we make the following assumption:

- Only the 2-D space is considered for reverse localization here. The location of the access point is determined in XY-coordinates, and 3-D localization is left for future work.
- The system assumes that the antennas are placed vertically on the Access Point, and are not tilted or bent in any way.
- While using Wi-Fi localization, we assume that the Transmitter and Receiver are synchronized in Time and Frequency, but not in phase.

3.3 Reverse Localization Algorithm

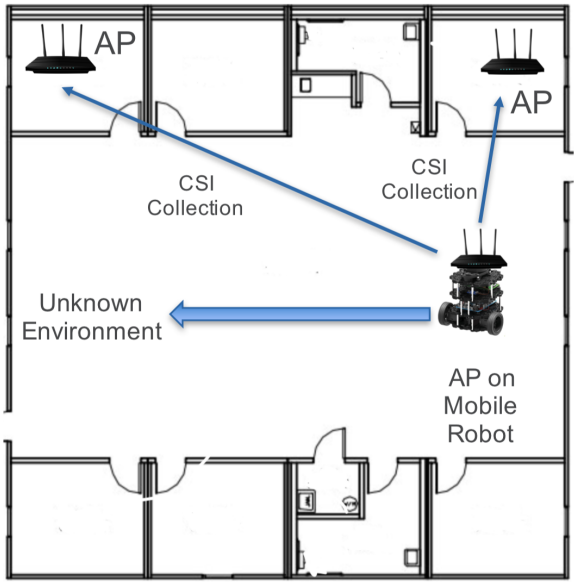

Figure 3.1: Robot traversing an unknown environment, and mapping it. It also collects CSI data during traversal

As mentioned previously, conventional localization assumes and requires prior knowledge of the locations of the APs in the indoor environment, and also their orientation and antenna separation. However, in an unknown environment, when we want to perform reverse localization, that will not be the case. Thus, when we look at the system requirements, we see that we require a map of the unknown environment, and to reverse localize the exact positions of the APs in this map. For creating the map of the unknown environment, a mobile robot which is able to navigate an unknown environment completely autonomously, and create a map of it is required. After creating this map, the robot localizes itself within the map. In order to obtain CSI data from all the access points, we need to mount an access point on to the robot, so that it can collect CSI data while its traversal and mapping of the unknown region.

Figure 3.2: Procedure flow, and a sample map obtained by the mobile robot traversing an unknown environment

One thing which we must consider before building a prospective system for reverse localization, is the level of accuracy that we require the location estimates to be. As observed in Figure 3.3, we can see that the median localization error increases drastically if the error in the APs location is greater than 0.1 meters. From this, we can infer that the required localization accuracy should be in the range of centimeters.

All of aforementioned WiFi based localization algorithms report increasing location accuracy with increase in the number of access points deployed in an environment. Based on this reasoning, we perform simple simulations where the number of access points in an indoor environment are increased linearly for a fixed set of 100 points in the environment. For this, the

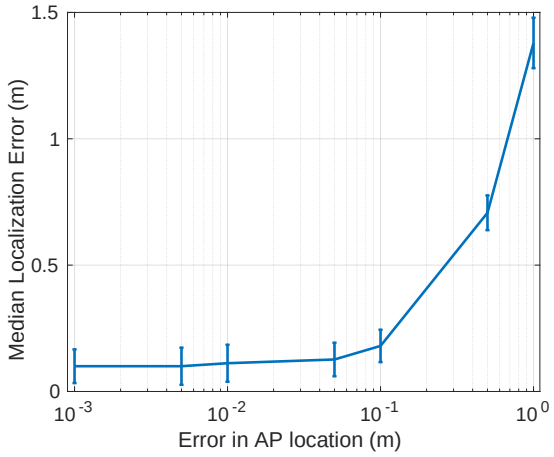

Figure 3.3: Increase in Median Localization error corresponding to error in estimated AP location

median localization accuracy achieved by the AoA based localization algorithms are reported in Figure 3.4.

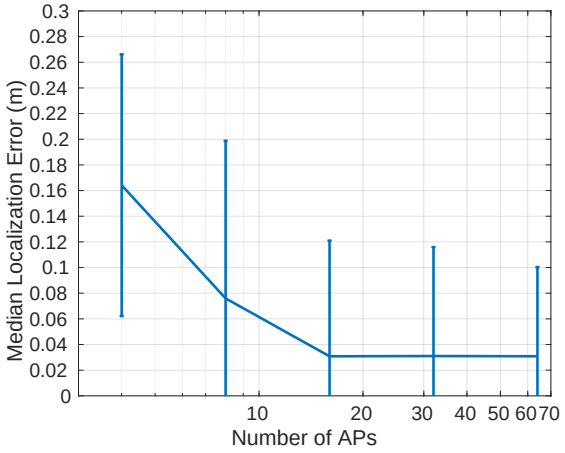

Figure 3.4: Decrease in median localization error with increase in number of Access points, asymptotically converging at 3cm

From this plot, we can observe that we can bring down the localization accuracy for these AoA based WiFi localization algorithms to centimeter level accuracy. While these results are inspiring, one cannot expect to deploy 10s of access points in an indoor environment. Where the

most access points deployed in any indoor environment are 4-6 and anymore APs would not be economical.

In a real-world case scenario, we can expect 3-4 APs to be present in the vicinity, which can enable us to get decimeter level localization accuracy at best, which is not accurate enough for reverse localization.

The way this problem is solved in our system, to achieve centimeter level accuracy can be observed in Figure 3.5. Since the robot is aware of its location, it can move in a fixed path across the environment in question and collect CSI data at different points. Since data collection is done at different points using the Access Point mounted on top of the robot, it essentially can simulate hundreds of APs if it collects data from multiple points. This enables the system to achieve its goal of providing centimeter-level localization accuracy to localize the Access Points in the region.

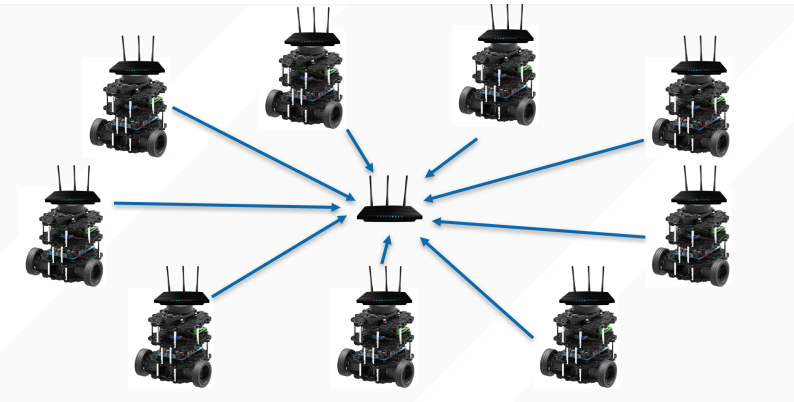

Figure 3.5: Simulating multiple Access Points by collecting CSI data at different points using the AP mounted on the mobile robot

This is similar to a Synthetic Aperture Radio (SAR). Though past works [6] solves for a renewed SAR problem with hand-held devices and achieve decimeter level localization accuracy, we take the advantage of the ground truth provided by the bot. Thus with the knowledge of the exact position and orientation of the transmitting antenna array, our system combines information across these hundreds of virtual anchors to accurately locate a single antenna on an access point

to centimeter level accuracy.

Further, reflected components of the multipath in an environment across these multiple virtual anchors would not be consistent. But the direct path across all these virtual anchors would give a singular solution. Thus we can see that the likelihood profile, $\sum_{i=1}^{N_a} \Lambda_i(\theta_m, L_k)$ (where $\Lambda_i(\theta_m, L_k)$ is the likelihood profile for the i^{th} virtual anchor among the N_a virtual anchors), would be relatively stronger only for the direct path than for any other reflected components of the multipath. Thus, the system also solves for multipath rejection to locate a single antenna exactly to a centimeter level accuracy.

Hence, we can observe that the process can be inverted, where all the APs in the environment act as user devices, and the mobile robot with the AP mounted on top of it acts like hundreds of APs in the environment, whose positions are known. We also know the orientation and antenna separation of the AP mounted on the mobile robot, thereby enabling us to utilize these algorithms. The next step after reverse localization would be to determine the antenna separation, and orientation of the said reverse localized AP.

In order to achieve this, the simpler solution would be if we can just simulate thousands of virtual APs with our autonomous robot and localize all the other antennas present on the AP to be localized, in the immediate region surrounding the first antenna. This enables us to obtain centimeter level accuracy for the locations of the other antenna, which in turn gives us centimeter-level accuracy for antenna separation. The key question here is, is centimeter-level accuracy for antenna separation enough to achieve good localization accuracy? The answer to that can be observed in Figure 3.6.

As seen in the plot, we can see that the median localization error is even more sensitive to small changes in the value of antenna separation. In order to achieve good localization accuracy, the error in this value should be in the order of millimeters. Also, it can be clearly seen that the median localization error saturates to $3cm$ just after 15 APs, as seen from Figure 3.3. This illustrates that localizing each individual antenna of the AP is not a viable prospect.

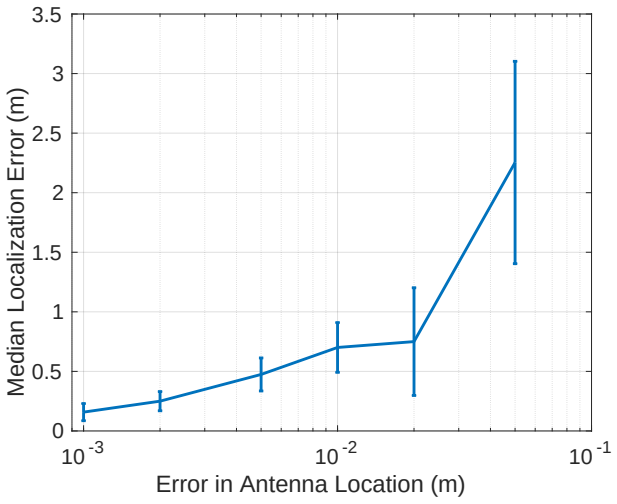

Figure 3.6: Increase in Median Localization error corresponding to error in estimated Antenna Separation

To overcome this limitation, we just locate one of the antennas on each AP. This gives us the cm-level localization accuracy for each AP. Then we locate the rest of the antennas with respect to this antenna, which we will refer to as the first antenna of the given AP. The next chapter describes how out system solves for the exact relative antenna positions on the AP with respect to first antenna and achieve millimeter-level localization accuracy.

Chapter 3 is adapted from material currently being prepared for submission for publication with Ganesaraman, Shreya; Rajagopalan, Shrivatsan; Ayyalasomayajula, Sai Roshan; Jain, Ish Kumar; Bharadia, Dinesh.

Chapter 4

Determination of AP Orientation and Antenna Separation

Now that one antenna on the unknown AP is localized, we need to know the locations of the other antennas present in its antenna array as well. One point to be noted here is that, we require millimeter-level accuracy when we determine the distance of separation between the antennas, due to the fact that it is already a very small number. This challenge can be overcome by means of looking at the relative channel information between two antennas present in the AP. This information does not vary heavily with time, and can provide fine, accurate estimates of the antenna separation and orientation of the AP under consideration.

The relative phase difference measured for an antenna at a distance d (antenna separation) away from the localized first antenna, when the incident angle-of-arrival is, θ, is given as follows when we consider direct path alone:

$$\Delta\phi = \mod\left(\frac{2\pi d}{\lambda}\sin(\psi+\theta), 2\pi\right) \tag{4.1}$$

As mentioned previously, this relative phase measured at the same access point, does not have any phase errors due to hardware and synchronization mismatches between the transmitter and the receiver. This leaves us with just the phase noise introduced by the hardware on the AP.

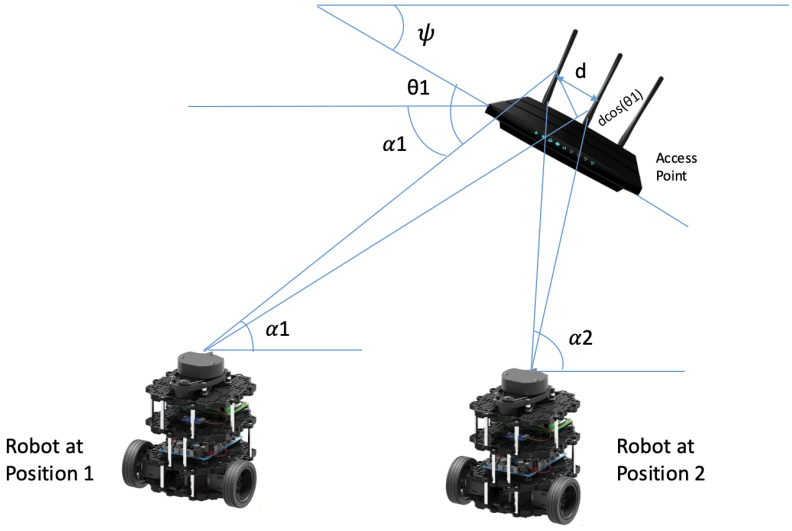

Figure 4.1: Diagrammatic representation of the closed form solution, considering two antennas at the AP, and the mobile robot at two different positions

To determine the exact location of the second antenna with respect to the first antenna, we need to solve for the x and y co-ordinates of the antenna with respect to the first antenna. Another thing to be considered here is that there are multiple reflections in an indoor environment, thus each resulting in it's own angle of arrival and it's own relative phase difference. to overcome this issue, we implement a multipath rejection algorithm similar to [9] and identify the direct path and make use of the phase difference corresponding to just the direct path. Once, we extract the phase difference corresponding to just the direct path we can solve for the relative position of the second antenna with respect to the first antenna.

Consider an unknown AP in the environment, oriented at an angle of ψ to the axis, and with antenna separation of d as shown in Figure 4.1. These variables are the unknowns that need to be solved in this case. From each position at the mobile robot is located at in the environment,

we get two key values, namely the AoAs α_1 and α_2, and the phase difference between the signals $\Delta\phi$ received by the Rx antennas 1 and 2 at the AP. We consider values reported by only one antenna of the AP mounted on the mobile robot at a time.

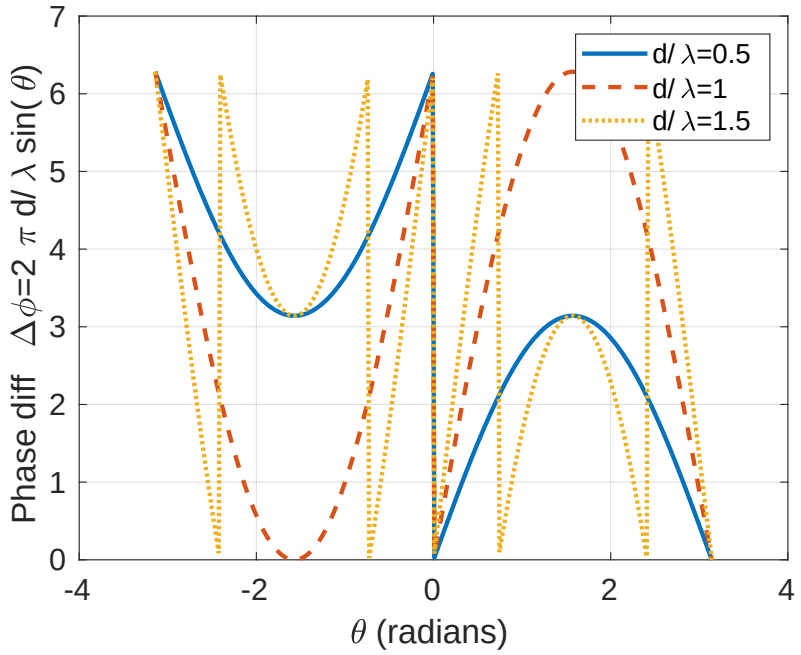

Figure 4.2: Estimating AoD from phase difference, by looking at the variation of phase difference with the AoD value θ

For each position i of the bot, we measure the CSI at the two antennas of the AP and obtain the phase difference between those antennas as:

$$\Delta\phi_i = \mod\left(\frac{2\pi d}{\lambda}\sin(\psi+\theta_i), 2\pi\right), \quad \forall i = 1,\ldots,L. \tag{4.2}$$

where θ_i is the AoD from the AP which is unknown at i^{th} position of the bot along the circular arc. Since $\Delta\phi_i$ is clipped to the range $[0, 2\pi]$, we can observe that multiple solutions are possible for ψ for $d > \lambda$ as shown in Figure 4.2. Now this makes the relative position of the second antenna not uniquely solvable. To overcome this problem, an interesting observation is

made that even though the phase difference is not unique over the entire range of angles, the rate of phase difference change is unique as shown in Figure 4.3. Hence, we leverage the set of measurements obtained at two locations of the bot to resolve the accurate relative location of the second antenna uniquely. We show that although there is one-to-many mapping from $\Delta\phi$ to ψ, the slope $\frac{d\Delta\phi}{d\theta}$ can provide a unique solution for θ as follows:

$$\frac{d\Delta\phi}{d\theta} = \frac{2\pi d}{\lambda}\cos(\psi+\theta) \tag{4.3}$$

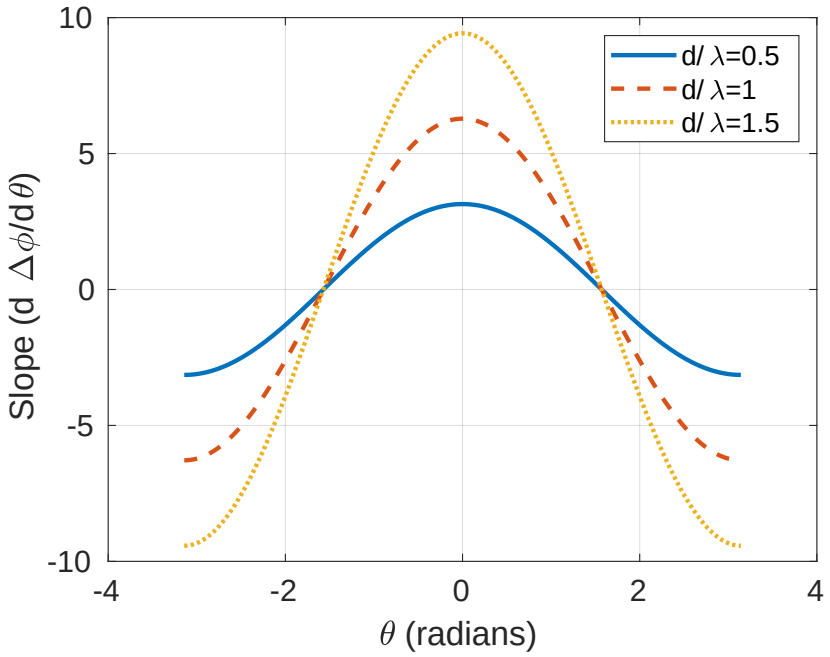

Figure 4.3: Estimating AoD from rate of change of phase difference, by looking at the variation of changes phase difference with the AoD value θ

Therefore, we obtain the estimate of (d,ψ) by estimating the slope $\frac{d\Delta\phi}{d\theta}$ (4.3)

$$\frac{d\Delta\phi_i}{d\theta} \approx \frac{\Delta\phi_{i+1}-\Delta\phi_i}{\theta_{i+1}-\theta_i} \tag{4.4}$$

The above approximation works especially well when the bot moves along a direction perpendicular to the Line-of-Sight(LOS) path. Now to solve for (d,ψ) uniquely we fix the origin

at the first antenna of the AP and represent the coordinate of the second antenna by its x and y coordinates:

$(x,y) = (d\cos(\psi), d\sin(\psi))$. We can then rewrite (4.3) in terms of (x,y) as follows:

$$\frac{d\Delta\phi_i}{d\theta} = 2\pi(x\cos(\theta_i) - y\sin(\theta_i)) \tag{4.5}$$

In vector form, we can rewrite the following set of linear equations in (x,y)

$$A\begin{bmatrix} x \\ y \end{bmatrix} = \mathbf{b} \tag{4.6}$$

where $A(i,:) = \begin{bmatrix} \cos(\theta_i) & -\sin(\theta_i) \end{bmatrix}$ and $\mathbf{b}_i = \frac{1}{2\pi}\frac{\Delta\phi_{i+1}-\Delta\phi_i}{\theta_{i+1}-\theta_i}$. Denote $\mathbf{x} = \begin{bmatrix} x & y \end{bmatrix}^T$. Note that we need at least three measurements of $(\theta_i, \Delta\phi_i)$ for $i = 1,2,3$ to get a unique solution for (x,y). In general, we collect a large number of samples and solve the following over-determined system of equations thus reducing the noise in the location estimates resulting in mm-level accurate location estimates.

$$\min_{\mathbf{x}} \quad ||A\mathbf{x} - \mathbf{b}||^2 \tag{4.7}$$

Finally we get (d,ψ) from $\mathbf{x}$ as follow

$$d = ||\mathbf{x}||, \text{ and } \psi = \angle\mathbf{x} \tag{4.8}$$

Note that the two measurements $\{\theta_i, \Delta\phi_i\}$ and $\{\theta_{i+1}, \Delta\phi_{i+1}\}$ should not be very close to avoid noise amplification. On the other hand, the measurements should not be very far away to cause error in the estimation of the derivative. Our experiment suggests that around 10^o of

angular separation $\theta_{i+1} - \theta_i$ provides the best results. The estimated value of ψ will be in the range of $0 \leq \psi \leq \pi$. We emphasize that we do not need to solve for ψ outside this range because the orientation of the antenna array can be defined uniquely in $0 \leq \psi \leq \pi$ since the orientation of antenna array can be defined uniquely in this range.

Chapter 4 is adapted from material currently being prepared for submission for publication with Ganesaraman, Shreya; Rajagopalan, Shrivatsan; Ayyalasomayajula, Sai Roshan; Jain, Ish Kumar; Bharadia, Dinesh.

Chapter 5

Experimental Setup and Evaluation

5.1 Requirements

The initial phase of Reverse Localization involves a mobile robot traversing an unknown environment. We utilize such a method because it is imperative to know the ground truth with respect to the user's position in order to initially localize the APs. Even though we can obtain large amounts of CSI data using crowdsourcing, the lack of ground truth for those renders them unusable for localization. Thus, a robot is used, and the major requirements of the mobile robot are as follows:

- Obtain a map of the environment in an autonomous manner, without any manual human intervention.
- The map thus obtained must be as accurate as possible, with a proper coordinate system and ground truth data, to enable ease of localization.
- The robot should be able to collect CSI data at regular time intervals during its traversal. This data must be clean and reliable, with minimal interference from ground reflections (possibly with the robot's antennas raised slightly from the ground).

With all these factors taken into consideration, the hardware platform chosen for mapping the environment and collecting Wi-Fi CSI data is chosen to be a mobile robot which utilizes the Simultaneous Localization And Mapping (SLAM) Algorithm [14, 16] for mapping the unknown region. This is one of the most widely used techniques for both indoor and outdoor mapping.

5.1.1 SLAM Algorithm

At a high level, the SLAM algorithm implemented in the mobile robot, as the name suggests, is used for localizing the robot traversing in the unknown environment, and mapping of the said environment simultaneously. At first sight, it can be considered as a chicken and egg problem, because we need accurate location for mapping, and vice versa. But there are many techniques to achieve it, by means of utilizing Kalman Filters, Probabilistic Estimates etc. Wi-Fi has been used in tandem with SLAM previously [16, 17]. In this case however, the main functionality in a hardware point of view, is achieved by means of using a LiDAR and Odometry. SLAM obtains data from the LiDAR and the Odometry data over time, and combines this to map the environment and localize itself as well. Out platform uses the Turtlebot 3 [4], a commodity mobile robot which uses LiDAR and Odometry based SLAM to map the required regions.

5.1.2 Turtlebot 3

The Turtlebot 3 is a commercially available mobile robot, whose main functions are SLAM, Navigation and Manipulation. It can be controlled remotely and used to navigate around a region. The Turtlebot 3 has a 360 degree LiDAR attached to it, along with multiple sensors including one for Odometry Data. The computing and control of the Turtlebot is handled by a Raspberry Pi 3 board. This robot utilizes the Robot Operating System (ROS) for its programming and functionality. Even though there are other, more expensive robots capable of SLAM and Navigation with highly accurate LiDARs, in order to keep the costs under control as well as

comply with the requirements of the system, the chosen robot was the Turtlebot 3. There are two techniques through which SLAM can be implemented using hardware - Cartographer and gmap.

The Turtlebot 3 was assembled, and ROS was installed in the robot and a remote computer with which it could also be controlled in addition to its autonomous movement. Gmap was setup in this robot in order to map the required region, with inputs from the 360-degree LiDAR and Odometry values. The ROS is launched after the hardware is setup, and TeleOp and RViz are used to control, navigate and view in real-time the map created by the robot.

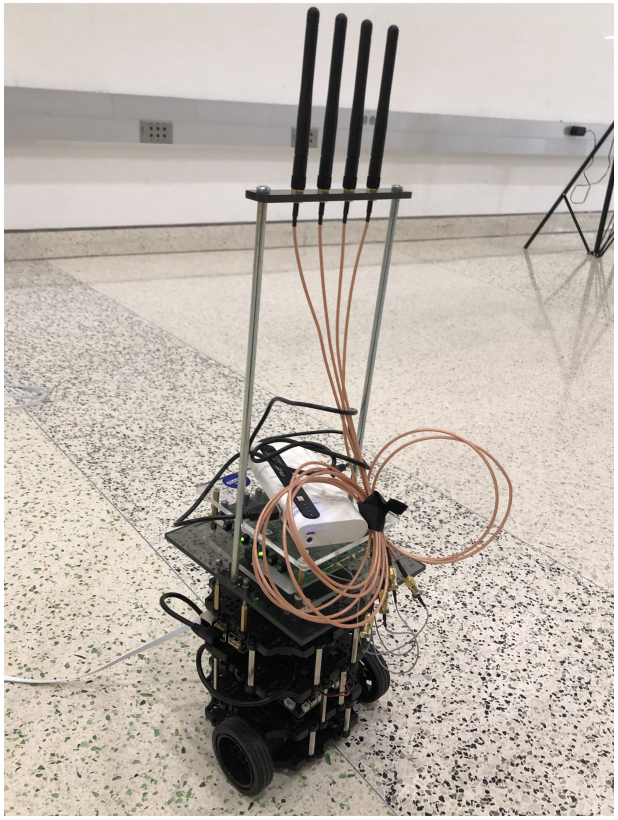

Figure 5.1: Turtlebot 3 Quantenna AP mounted on it

In order to obtain CSI data from all the access points, we need to mount an access point on to the Turtlebot 3, so that it can collect CSI data while its traversal and mapping of the unknown region. Thus, a Quantenna[34] AP was mounted on top of the Turtlebot 3. This Quantenna can be controlled remotely as well by the user, through the Raspberry Pi 3 board present in the Turtlebot.

The Quantenna is setup in such a way that it can send small amounts of data to all the APs present in the region. Due to this packet communication, it is able to measure Channel State Information (CSI) values. These values are obtained by transmitting a small amount of data packets from the AP mounted on the robot, to all the surrounding APs in the considered region.

Using these transmissions, the CSI values are calculated per antenna per subcarrier, and can be collected either at each of the Access Points or the AP present on the robot. This information is then extracted and utilized to run all the reverse localization algorithms.

The Quantenna Wi-Fi card APs were also utilized as the AP stations placed at random locations in the environment. The data parameters collected by the AP placed on the Quantenna are the CSI data, RSSI, hardware noise, bandwidth, local timestamp, MCS and the number of transmitting and receiving antennas. Some of the issues identified on using this setup are found to be as follows:

- Due to the fact that many of the commodity AP stations are placed near the roof, and in general are at a height much higher than the ground, we can see that ground reflections can significantly affect the data collected by the robot. This can be overcome by raising the height of the antenna array present in the robot as much as possible. We have done the same thing using acrylic cut sheets and metallic rods to a reasonable height without compromising on the stability of the robot. This enabled us to obtain much cleaner data.

- Also, due to the height factor, another issue is the 3D offset. This can also be overcome by lifting the antennas to a certain level, as mentioned previously. Quite a significant improvement was observed in the quality of the data with minimized 3D and ground reflections when this was practically implemented.

- Another major problem is the issue of time synchronization between the robot and the AP mounted on the robot. The timestamps reported by the CSI values obtained using the AP are based on the internal on-chip clock present in it. This reports timestamps relative to the

power-on duration of the AP, and not the actual time values. On the other hand, the robot's timestamps are based on Unix epoch times reported by it along with its ground truth while running ROS. This synchronization problem can be overcome by considering a sample CSI packet, and comparing the corresponding epoch timestamp to synchronize them from that point onward. This time synchronization is done just before the data collection to make sure that the synchronization is maintained right from the start.

Thus, a hardware platform with a Turtlebot 3 running SLAM for mapping and navigation, with a station mounted on it to obtain CSI data from the APs in that region is designed and implemented. This platform was used to collect CSI data for the reverse localization.

5.2 Reverse Localization Procedure and Evaluation

As mentioned previously, the Quantenna AP mounted on top of the Turtlebot 3 is deployed into the environment. There are also other Quantenna AP stations present at arbitrary locations in the region. The robot is first time synchronized with the AP mounted on top of it, and begins its exploration from a predetermined start point. This is achieved by powering on the robot, running the initial setup and time synchronization scripts and then accessing the Robot Operating System (ROS) to be able to control the robot's motion and observe the map generated by the robot in real time as well. The Turtlebot 3 uses the LiDAR and odometry data to run its SLAM algorithm and starts creating a map of the region. On traversing through the entire environment, we can obtain a map as a result. Within this map, the robot is able to localize itself.

5.2.1 Data Collection and Reverse Localization

After the map is obtained, the robot moves back to its start point, or any known point in the map. From this position, the robot once again traverses the region to collect CSI data at regular intervals. To collect this data, the robot moves a given distance in a given time interval,

stops, collects the CSI data using the appropriate data collection scripts, and continues its motion. By making the robot traverse slowly, a large amount of CSI data can be collected for the said region in question. This process is repeated until the entire region is completely traversed, and a large amount of CSI data is obtained.

The multipath profile of the received signals are computed from the CSI data, and we obtain location estimates for the AP in the environment, at each position where the robot collected CSI data. These estimates are aggregated from multiple positions, and the most likely location of the first antenna of each of the APs present in the region is determined. Thus, we can get location estimates in the coordinate form based on the robot's map for all the APs. Thus, reverse localization is successfully achieved.

5.2.2 Results

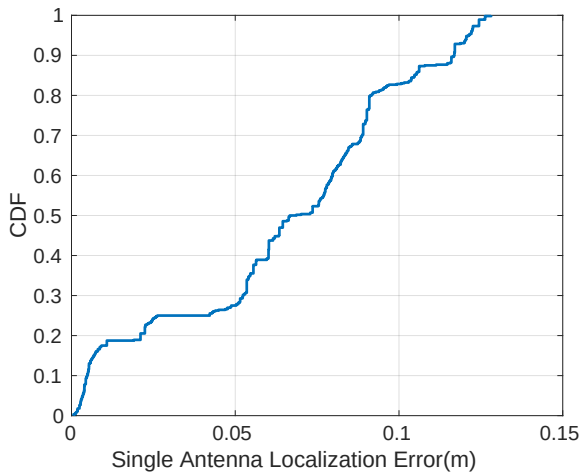

Figure 5.2: CDF Plot for Reverse Localization Accuracy for localization of a single antenna

For testing the reverse localization, we consider a testbed with a Quantenna AP placed at a random location, and the mobile robot is allowed to traverse this environment, and collect CSI data at multiple points. For reverse localizing a single antenna of an AP in a real-world

environment, we placed multiple Quantenna APs at different heights, and the reverse localization algorithm was implemented using the collected CSI data. The CDF plot for the localization error can be seen in Figure 5.2. We can observe that the median localization error is well within the expected centimeter level of localization accuracy that we expect from the system. This enables us to determine the antenna separation accurately, and thereby provide good accuracy in forward localization as well.

Various other experiments were performed to test the accuracy and robustness of the system. By varying the number of antennas of the station mounted on the robot between 2-4, the CDF plot of the localization accuracy as a result can be observed in Figure 5.3. We can see that with more antennas present on the robot, the better median localization accuracy we obtain.

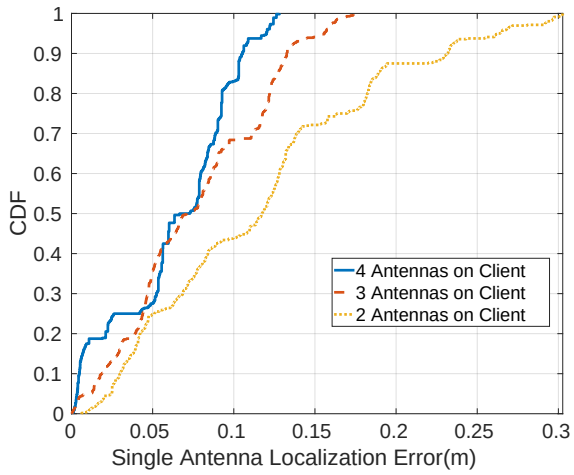

Figure 5.3: CDF Plot for Reverse Localization Accuracy for localization of a single antenna, with varying number of antennas present on the station mounted on the robot

The bandwidth of operation was also varied between 20-80 MHz, and the CDF plots for the localization error across different bandwidths can be seen in Figure 5.4. We can observe good localization accuracy at 80 MHz, and the error progressively increases as the bandwidth decreases to 20 MHz.

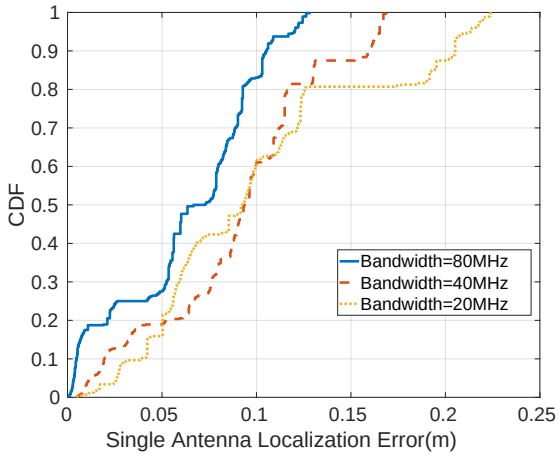

Figure 5.4: CDF Plot for Reverse Localization Accuracy for localization of a single antenna, with varying bandwidths of operation

5.3 AP Geometry Prediction Results

Using the AP's estimated location, we need to determine the locations of the other antennas relative to the first antenna. As mentioned previously, localizing each antenna individually does not give us the required level of accuracy, and hence we look at the relative phase information between the two antennas.

Once again, we have considered a similar testbed to implement our algorithm for determining AP's geometry. Using the collected CSI data and the location estimates, we have obtained the values for the locations of the other antennas relative to the first antenna which was localized. These experiments were performed for different antenna array geometries like a linear antenna array, rectangular antenna array etc. The CDF plot for antenna localization error can be observed in Figure 5.5.

As observed from the Figure 5.5, we have a median localization error of in the range of a few millimeters for the predicted antenna locations. This is within out desired threshold of millimeter-level accuracy required to design a robust forward localization system.

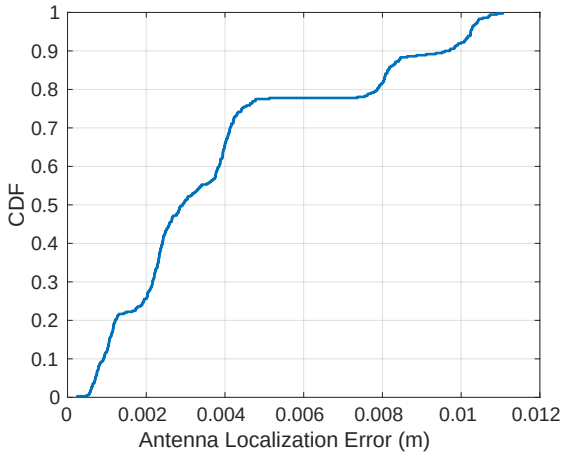

Figure 5.5: CDF plot for error in predicted values of antenna separation d

5.4 Error in Reported Ground Truth

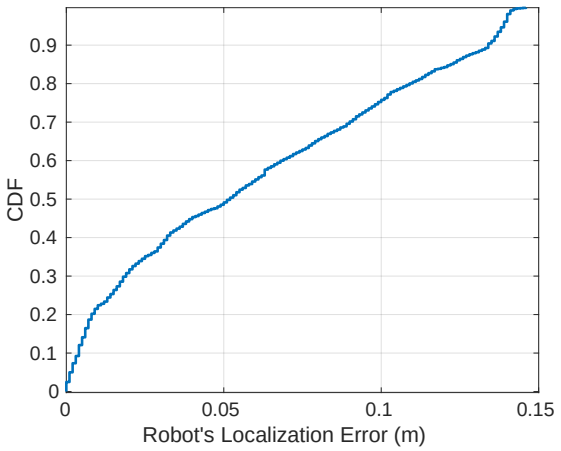

Figure 5.6: The CDF plot of the error in ground truth reported by the mobile robot

Since we are dependent on the Ground Truth values reported by the robot to achieve reverse localization. Hence it is imperative to note and take into account the drift of the ground truth values reported by the robot. In order to evaluate this, we made the robot traverse through a trajectory whose ground truth was known, and compared it with the ground truth values reported by the mobile robot. The CDF plot for the error in reported ground truth values can be observed

in Figure 5.6. As observed, there are some errors in the reported ground truth values due to drift over time and the nature of the environment, with the median error in reported ground truth in the order of 5-6 cm. However, by collecting CSI data at multiple points in the environment, we are able to overcome this drift and arrive at the desired level of accuracy required for the system.

Chapter 5 is adapted from material currently being prepared for submission for publication with Ganesaraman, Shreya; Rajagopalan, Shrivatsan; Ayyalasomayajula, Sai Roshan; Jain, Ish Kumar; Bharadia, Dinesh.

Chapter 6

Conclusion and Future Work

6.1 Summary

Reverse Localization of Access Points has been achieved successfully. Also the need for orientation and antenna separation is discussed, and those were determined as a result of the Closed Form method and the Arc method. The main contributions are as follows:

- Centimeter-level accuracy for the reverse localization of Access Points was obtained.
- An error of under 10 degrees was observed for the predicted orientation of the Access Points.
- Millimeter-level accuracy was obtained for the predicted values of antenna separation was obtained.

6.2 Future Work

The next part of this system will be extensive stress testing in more strenuous testbeds with multiple APs and strong multipath. The accuracy of the system in such adverse conditions needs to be tested. This is being currently done.

One major future work for this system would be to make this reverse localization work for APs whose antenna geometries are arbitrary and do not follow any shape or pattern. Also, to further improve the accuracy of localization and reverse localization we can use more advanced robots and highly sensitive APs mounted on it.

Another interesting problem would be to design a similar reverse localization system which could work in 3D. Here, the height at which the Access Points are present could also be determined to further improve indoor localization accuracy.

6.3 Applications

As a result of this system, we can obtain APs which are self-aware about their location, thereby enabling them to know the exact location of a user device in the given environment. The prospective applications of this are exciting. For example, when the user wishes to navigate to a particular store in a shopping mall, a UI-based app using Wi-Fi can be opened, and the users location can be determined inside the building. By using pre-programmed information about the locations of all the stores present in the mall, a navigation system can be designed using the map and location information. The user can then be guided to the required destination by using interactive graphics and animations.

Chapter 6 is adapted from material currently being prepared for submission for publication with Ganesaraman, Shreya; Rajagopalan, Shrivatsan; Ayyalasomayajula, Sai Roshan; Jain, Ish Kumar; Bharadia, Dinesh.

Bibliography

[1] Global Positioning System - Information. http://www.gps.gov.

[2] Google Maps. www.maps.google.com.

[3] Robot Operating System. www.ros.org.

[4] Turtlebot 3 Specifications. http://www.robotis.us/turtlebot-3/.

[5] Uber. www.uber.com.

[6] VICON T-Series. www.vicon.com/products/documents/Tseries.pdf.

[7] Fadel Adib, Zach Kabelac, Dina Katabi, and Robert C. Miller. 3D Tracking via Body Radio Reflections. NSDI, 2014.

[8] Fadel Adib, Zachary Kabelac, and Dina Katabi. Multi-person Localization via RF Body Reflections. NSDI, 2015.

[9] Roshan Ayyalasomayajula, Deepak Vasisht, and Dinesh Bharadia. Bloc: Csi-based accurate localization for ble tags. In *Proceedings of the 14th International Conference on emerging Networking EXperiments and Technologies*, pages 126–138. ACM, 2018.

[10] Martin Azizyan, Ionut Constandache, and Romit Roy Choudhury. Surroundsense: Mobile phone localization via ambience fingerprinting. In *Proceedings of the 15th Annual International Conference on Mobile Computing and Networking*, MobiCom '09, pages 261–272, New York, NY, USA, 2009. ACM.

[11] Victor Bahl and Venkat Padmanabhan. RADAR: An In-Building RF-based User Location and Tracking System. INFOCOM, 2000.

[12] Krishna Chintalapudi, Anand Padmanabha Iyer, and Venkata N. Padmanabhan. Indoor Localization Without the Pain. MobiCom, 2010.

[13] Carmelo Di Franco, Amanda Prorok, Nikolay Atanasov, Benjamin Kempke, Prabal Dutta, Vijay Kumar, and George Pappas. Calibration-free network localization using non-line-of-sight ultra-wideband measurements. In *CVPR*, 2017.

[14] H. Durrant-Whyte and T. Bailey. Simultaneous Localisation and Mapping (SLAM): Part I The Essential Algorithms. IEEE Robot. Autom.Mag, 2006.

[15] Jon Gjengset, Jie Xiong, Graeme McPhillips, and Kyle Jamieson. Phaser: Enabling Phased Array Signal Processing on Commodity Wi-Fi Access Points. *MobiCom*, 2014.

[16] Zakieh Sadat Hashemifar, Charuvahan Adhivarahan, and Karthik Dantu. Improving rgb-d slam using wi-fi. In *Proceedings of the 16th ACM/IEEE International Conference on Information Processing in Sensor Networks*, pages 317–318. ACM, 2017.

[17] Joseph Huang, David Millman, Morgan Quigley, David Stavens, Sebastian Thrun, and Alok Aggarwal. Efficient, generalized indoor wi-fi graphslam. In *Robotics and Automation (ICRA), 2011 IEEE International Conference on*, pages 1038–1043. IEEE, 2011.

[18] Vikram Iyer, Vamsi Talla, Bryce Kellogg, Shyamnath Gollakota, and Joshua Smith. Inter-technology backscatter: Towards internet connectivity for implanted devices. In *SIGCOMM*, 2016.

[19] Kiran Joshi, Steven Hong, and Sachin Katti. PinPoint: Localizing Interfering Radios. NSDI, 2013.

[20] Bryce Kellogg, Aaron Parks, Shyamnath Gollakota, Joshua R Smith, and David Wetherall. Wi-fi backscatter: Internet connectivity for rf-powered devices. In *ACM SIGCOMM Computer Communication Review*, 2014.

[21] Bryce Kellogg, Vamsi Talla, Shyamnath Gollakota, and Joshua R Smith. Passive wi-fi: Bringing low power to wi-fi transmissions. In *NSDI*, 2016.

[22] Manikanta Kotaru, Kiran Joshi, Dinesh Bharadia, and Sachin Katti. SpotFi: Decimeter Level Localization Using Wi-Fi. SIGCOMM, 2015.

[23] Manikanta Kotaru and Sachin Katti. Position tracking for virtual reality using commodity wifi. In *CVPR*, 2017.

[24] Manikanta Kotaru, Pengyu Zhang, and Sachin Katti. Localizing low-power backscatter tags using commodity wifi. In *CoNEXT*, 2017.

[25] Swarun Kumar, Stephanie Gil, Dina Katabi, and Daniela Rus. Accurate Indoor Localization with Zero Start-up Cost. MobiCom, 2014.

[26] Swarun Kumar, Ezzeldin Hamed, Dina Katabi, and Li Erran Li. LTE Radio Analytics Made Easy and Accessible. SIGCOMM, 2014.

[27] Hyuk Lim, Lu-Chuan Kung, Jennifer C. Hou, and Haiyun Luo. Zero-configuration, robust indoor localization: Theory and experimentation. *Proceedings IEEE INFOCOM 2006. 25TH IEEE International Conference on Computer Communications*, pages 1–12, 2006.

[28] Hui Liu, Houshang Darabi, Pat Banerjee, and Jing Liu. Survey of wireless indoor positioning techniques and systems. *IEEE Transactions on Systems, Man, and Cybernetics, Part C (Applications and Reviews)*, 37(6):1067–1080, 2007.

[29] Yunfei Ma, Nicholas Selby, and Fadel Adib. Drone relays for battery-free networks. In *SIGCOMM*.

[30] Yunfei Ma, Nicholas Selby, and Fadel Adib. Drone relays for battery-free networks. In *Proceedings of the Conference of the ACM Special Interest Group on Data Communication*, pages 335–347. ACM, 2017.

[31] Yunfei Ma, Nicholas Selby, and Fadel Adib. Minding the billions: Ultra-wideband localization for deployed rfid tags. In *MobiCom*, 2017.

[32] Rajalakshmi Nandakumar, Krishna Kant Chintalapudi, and Venkata N. Padmanabhan. Centaur: Locating devices in an office environment. In *Proceedings of the 18th Annual International Conference on Mobile Computing and Networking*, Mobicom '12, pages 281–292, New York, NY, USA, 2012. ACM.

[33] Dragoş Niculescu and Badri Nath. Vor base stations for indoor 802.11 positioning. In *Proceedings of the 10th Annual International Conference on Mobile Computing and Networking*, MobiCom '04, pages 58–69, New York, NY, USA, 2004. ACM.

[34] Quantenna. Quantenna 802.11ac WiFi Card.

[35] Anshul Rai, Krishna Kant Chintalapudi, Venkata N. Padmanabhan, and Rijurekha Sen. Zee: Zero-effort Crowdsourcing for Indoor Localization. MobiCom, 2012.

[36] Research Markets. Indoor Location Market worth 23.13 Billion USD by 2021, 2016. http://www.marketsandmarkets.com/PressReleases/indoor-location.asp.

[37] Chris Rizos, Gethin Roberts, Joel Barnes, and Nunzio Gambale. Experimental results of locata: A high accuracy indoor positioning system. In *Indoor Positioning and Indoor Navigation (IPIN), 2010 International Conference on*, pages 1–7. IEEE, 2010.

[38] Souvik Sen, Jeongkeun Lee, Kyu-Han Kim, and Paul Congdon. Avoiding Multipath to Revive Inbuilding Wi-Fi Localization. MobiSys, 2013.

[39] Elahe Soltanaghaei, Avinash Kalyanaraman, and Kamin Whitehouse. Multipath triangulation: Decimeter-level wifi localization and orientation with a single unaided receiver. In *MobiSyS*, 2018.

[40] Deepak Vasisht, Swarun Kumar, and Dina Katabi. Decimeter-Level Localization with a Single Wi-Fi Access Point. NSDI, 2016.

[41] Jue Wang, Fadel Adib, Ross Knepper, Dina Katabi, and Daniela Rus. Rf-compass: Robot object manipulation using rfids. In *Proceedings of the 19th annual international conference on Mobile computing & networking*, pages 3–14. ACM, 2013.

[42] Jie Xiong and Kyle Jamieson. ArrayTrack: A Fine-grained Indoor Location System. NSDI, 2013.

[43] Chenren Xu, Bernhard Firner, Yanyong Zhang, Richard Howard, Jun Li, and Xiaodong Lin. Improving RF-based Device-free Passive Localization in Cluttered Indoor Environments Through Probabilistic Classification Methods. IPSN, 2012.

[44] Moustafa Youssef and Ashok Agrawala. The Horus WLAN Location Determination System. MobiSys, 2005.

[45] Pengyu Zhang, Dinesh Bharadia, Kiran Joshi, and Sachin Katti. Hitchhike: Practical backscatter using commodity wifi. In *SenSys*, 2016.